ELSEVIER

Carbohydrate Research 304 (1997) 209–217

CARBOHYDRATE RESEARCH

Studies on the structure and the solution conformation of an acidic extracellular polysaccharide isolated from *Bradyrhizobium*

Ana Poveda [a], Mónica Santamaría [b], Manuel Bernabé [c], Alicia Prieto [d], Marta Bruix [e], Javier Corzo [b], Jesús Jiménez-Barbero [c,*]

[a] *Servicio Interdepartamental de Investigación, Universidad Autonoma de Madrid, Cantoblanco 28049 Madrid, Spain*

[b] *Departamento de Bioquímica y Biología Molecular, Universidad de la Laguna, 38071 Tenerife, Spain*

[c] *Instituto Quimica Organica, CSIC, Juan de la Cierva 3, 28006 Madrid, Spain*

[d] *Centro de Investigaciones Biológicas, CSIC, Velazquez, 28006 Madrid, Spain*

[e] *Instituto Estructura de la Materia, CSIC, Serrano 117, 28006 Madrid, Spain*

Received 31 March 1997; accepted 25 July 1997

Abstract

The structure of an acidic extracellular polysaccharide isolated from *Bradyrhizobium* (*Chamaecytisus proliferus*) has been elucidated by hydrolysis, methylation analysis, and 1D and 2D ^{1}H- and ^{13}C-NMR spectroscopy of the complete polysaccharide. The NMR spectrum showed that microheterogeneity was present due to the minor existence of a variety of O-acetyl groups. Thus, a deacetylated sample was prepared by alkaline treatment which was then fully analysed. The deacetylated polysaccharide has the following sequence:

→ 3)-[α-D-Gal*p*-(1 → 6)]-α-D-Glc*p*-(1 → 3)-β-D-Glc*p*-(1 → 3)-α-D-Gal*p*A-(1 → 3)-α-D-Man*p*-(1 →

The sample is partially O-methylated at position 4 of the α-D-Gal*p*-(1 → 6) unit. In addition, the same moiety of the native sample is also partially and heterogeneously O-acetylated. The conformational features of the deacetylated sample have been evaluated by molecular mechanics and dynamics calculations and NOE spectroscopy. The results indicate that the polysaccharide may adopt a variety of three dimensional shapes, and that there is a fair agreement between the NMR-derived distances and those provided by the calculations.

Keywords: Polysaccharide; NMR spectroscopy; Molecular modelling; *Bradyrhizobium*

* Corresponding author. Fax: +34-1-5644853; e-mail iqojj01@pinar1.csic.es.

0008-6215/97/$17.00
PII S0008-6215(97)00237-1

1. Introduction

Soil bacteria of the genus *Bradyrhizobium* are of interest because they are involved in the reduction of dinitrogen to ammonia in symbiosis with tropical and subtropical legumes, including soybean. These bacteria produce acidic polysaccharides whose physiological role is presently unknown, although it has been claimed that their involvement in the symbiotic process is due to specific binding to plant lectins. These bacteria secrete a variety of extracellular polysaccharides (EPS), and some of them are acidic [1]. It has been reported that the acidic polysaccharide produced by *Bradyrhizobium* (*Chamaecytisus*) BGA-1 precipitates with aqueous solutions of metallic cations as Fe^{3+} (but not Fe^{2+}), Al^{3+}, Sn^{2+}, and Th^{4+}. Therefore, it is possible, that this polysaccharide acts as defense against toxic metals present in the environment of the bacterium [2]. Different to other acidic polysaccharides, BGA-1 does not form gels in the presence of mono- or divalent cations. In addition, and interestingly, the acidic polysaccharide produced by a related bacteria, *B. japonicum* USDA110, is unable to precipitate with Al^{3+}, Th^{4+}, and Sn^{2+}, and it requires their previous deacetylation to precipitate with Fe^{3+} [3]. The mechanism of the specific precipitation of BGA-1 with cations and the basis of its different behaviour remains unknown. This paper presents the full characterization of the acidic extracellular polysaccharide isolated from *Bradyrhizobium* (*Chamaecytisus*) strain BGA-1 using modern NMR techniques and methylation analysis. In addition, the three dimensional structure of the polysaccharide has been studied by NMR and molecular modelling, as a first step to determine the influence of its conformation in their particular ecological and practical properties [4].

2. Experimental

Materials.—Culture of the bacteria and purification of the extracellular acidic polysaccharide were performed as previously described [2].

Reduction of the polysaccharide.—The uronic acids were detected in the NMR experiments and then, the polysaccharides were reduced according to the method of Taylor and Conrad [5], using $NaBD_4$.

Methylation analysis.—The reduced samples were methylated following the method of Ciucanu and Kerek [6]. The methylated polysaccharides were hydrolysed and the monosaccharides released were converted into partially methylated alditol acetates and then analysed by GC–MS, using a SPB-1 column.

Molecular mechanics and dynamics calculations.—Molecular mechanics and dynamics calculations were performed using both the CVFF force field [7] within the INSIGHT II/DISCOVER programs of BIOSYM technologies (San Diego, CA) and the MM3* force field as implemented in MACROMODEL 4.5 [8]. Φ is defined as H-1′–C-1′–O-1′–C–*X* and Ψ as C-1′–O-1′–C–*X*–H–*X*, except for the $1 \rightarrow 6$ linkage, which is defined as C-1′–O-1′–C-6–C-5. Thus, the atoms of the non-reducing end are primed. Only the *gg* orientation of the lateral chain was used for the β-Glc, α-GlcA and α-Man moieties, while the *gt* conformation were used for the non-reducing α-Gal residue. However, for the $1 \rightarrow 6$ linkage, both gg and gt rotamers were considered for the α-Glc moiety. A dielectric constant $\epsilon = 80$ was used. First, potential energy maps were calculated for every individual constituent disaccharide: relaxed (Φ, Ψ) potential energy maps were calculated as described [9]. In total, 400 conformers were calculated for every disaccharide and every force field. The previous step involved the generation of the corresponding rigid residue maps by using a grid step of 18°. Then, every Φ, Ψ point of this map was optimised using 200 steepest descent steps, followed by 1000 conjugate gradient iterations. From these relaxation maps, the probability distributions were obtained according to a Boltzmann function at 300 K [10].

A nonasaccharide model of the polysaccharide was built by combining the more stable conformers of the different glycosidic linkages and this was subjected to extensive energy minimization with conjugate gradients. The nonasaccharide contained two $1 \rightarrow 6$ linkages, with gg and gt rotamers, respectively. The final minimized structure was used as starting geometry for molecular dynamics (MD) simulations [11] in vacuo at 300 K, with a dielectric constant of 80, and a time step of 1 fs. The equilibration period was 100 ps. After this period, structures were saved every 0.5 ps. The total simulation time was 1 ns for every run. Average distances between intraresidue and inter-residue proton pairs were calculated from the dynamics simulations. Different simulations with both the MM3* and the CVFF force fields were performed.

NMR spectroscopy.—NMR experiments were recorded on Varian Unity 500 and Bruker AMX-300 spectrometers, using an approximate 15 mg/mL solution of the polysaccharide in D_2O at 299 K [12]. The estimated molecular weight is around 30 kDa.

Chemical shifts are reported in ppm, using the residual HDO signal (4.72 ppm) and external TMS (0 ppm) as references. The double quantum filtered COSY spectrum (500 MHz) was performed with a data matrix of 256 × 1K to digitize a spectral width of 2000 Hz. 16 scans were used with a relaxation delay of 1 s. The 2D TOCSY experiment was performed using a data matrix of 256 × 2K to digitize a spectral width of 2000 Hz; 16 scans were used per increment with a relaxation delay of 2 s. MLEV 17 was used for the 100 ms isotropic mixing time. The one-bond proton–carbon correlation experiment was collected in the ^{1}H-detection mode using the HMQC sequence and a reverse probe. A data matrix of was used to digitize a spectral width of 2000 Hz in F_2 and 10,000 Hz in F_1. 16 scans were used per increment with a relaxation delay of 1 s and a delay corresponding to a J value of 145 Hz. A BIRD pulse was used to minimize the proton signals bonded to ^{12}C. ^{13}C decoupling was achieved by the WALTZ scheme. The 2D-HMQC–TOCSY experiment was conducted (300 MHz) with no ^{13}C decoupling during acquisition and 80 ms of mixing time (MLEV 17). The same conditions as for the HMQC were employed. HMBC experiments were performed at 500 MHz with a data matrix of 256 × 2K to digitize a spectral width of 2000 × 15,000 Hz. 64 scans were acquired per increment with a delay of 65 ms for evolution of long range couplings.

Selective inversion of the anomeric protons was performed using the DANTE-Z module [13] during 60 ms. 1D-NOESY experiments were recorded using mixing times of 100, 150, 200, 250, and 300 ms. 1D-ROESY experiments used mixing times of 100, 200, 300, and 400 ms. The rf carrier frequency was set at δ 6.0 ppm, and the spin locking field was 2.5 KHz. 2D NOESY and 2D ROESY experiments were also performed with the same mixing times, and using 256 × 2K matrixes. Good linearity was observed up to 200 (NOESY) and 300 ms (ROESY). Estimated errors in the NOE intensities are smaller than 20%. DANTE-Z based 1D-TOCSY–NOESY were also performed.

3. Results and discussion

Structure elucidation.—The ^{1}H-NMR spectrum of the intact polysaccharide in water solution at 298 K contained six major signals in the anomeric region (Fig. 1). A number of minor signals were also evident in the 1D spectrum. In addition, small signals, one major and four minor singlet resonances were present around 2 ppm, probably belonging to O-acetyl groups, and one additional singlet appeared at 3.5 ppm, showing the possible presence of a O-methyl group. All these substitutions were evidently in minor proportion in the native polysaccharide (Fig. 1). In addition, the ^{13}C-NMR spectrum of the sample (Fig. 1) and the proton–carbon HMQC (Fig. 2) correlation experiments showed unequivocally the presence of these minor OMe and OAc groups. In order to facilitate the assignment of the primary sequence, by eliminating most of the microheterogeneities observed in the 1D NMR spectrum, the polysaccharide was deacetylated by treatment with diluted sodium hydroxide and amberlite. The resultant sample was lyophylised several times with D_2O and used for the NMR experiments without further purification.

The ^{1}H-NMR spectrum of the deacetylated polysaccharide (Fig. 1) contained 6 major anomeric protons, labelled A–F, as well as a singlet at 3.51 ppm (OMe). The signals at ca. 2 ppm did not appear in this sample. The integrals taken for protons A–F showed 1:1:1:0.66:0.33:1 ratios. The double quantum filtered COSY experiment allowed the assignment of all H-2 protons for every residue A–F. The combination of this experiment with the TOCSY correlation map (Fig. 2) provided the identification of additional resonance signals for residues A, B, C, and F. Strong overlap was observed for the proton signals of residues D and E. The ^{13}C-NMR spectrum, in combination with the HMQC correlation experiment (Fig. 2) also showed the presence of six anomeric carbons, although the ^{13}C resonances of residues D and E showed overlap. A signal at 175 ppm was also evident, indicating the possible presence of a COOH moiety. The combination of ^{1}H- and ^{13}C-NMR information [14] indicated that residues A–E were α, and F was β, since the anomeric protons of residues A–E resonated above 4.96 ppm and their corresponding carbons appeared at higher field than 102 ppm. On the other hand, the anomeric proton of F appeared at 4.71 ppm, and its connected carbon at 104.7 ppm.

At this point, information from sugar and methylation analysis was used. Monosaccharide analysis showed the presence of Glc, Man, Gal, and GalA in 2:1:1:1 molar ratios. Besides, methylation analysis indicated the presence of terminal Gal*p*, 3-O-substituted Man*p*, 3-O-substituted Glc*p*, and 3,6-O-substituted Glc*p*. When the carbonyl group was reduced and the resultant sample was submitted to subsequent analysis, the presence of 3-O-substituted Gal*p*A was also detected.

The combination of HMQC, HMQC–TOCSY, HMQC–NOESY (Figs. 2–4) and HMBC experiments allowed assignment of most of the signals of the deacetylated polysaccharide. In fact, all the resonances of residues A, B, C, and F were identified. The comparison of the observed ^{1}H- and ^{13}C-NMR chemical shifts [14] of these signals with those reported in literature allowed identification of A as 3,6-di-O-substituted α-Glc*p*, B as 3-O-substituted α-Gal*p*A, C as 3-O-substituted α-Man*p*, and F as 3-O-substituted β-Glc*p*. The information already available for residues D and E showed that α-Gal*p* were terminal moieties. NOESY and HMBC experiments allowed identification of the glycosidic connectivities. Thus, A-1 was shown to be connected to F-3, B-1 to C-3, C-1 to A-3, F-1 to B-3, and D-1 and E-1 to A-6. The difference between D and E is due to the presence of the OMe group at position 4 of residue E, as shown by the NOESY (cross peak OMe/E H-4), HMBC (cross peak CH_3, E C-4), and ^{13}C-NMR chemical shift information. Therefore, there are two different polysaccharides, the difference being O-methylation (33%) at position 4 of the terminal α-D-Gal*p* unit. NOESY experiments also allowed to confirm the α character of residues A–E (only H-1/H-2 intraresidue cross peaks) and the β nature of residue F (only H-1/H-3,H-5 intraresidue cross peaks). This NMR-based information (Table 1) is in good agreement with the methylation analysis experiments and indicates the following structure for the major deacetylated polysaccharide (66%):

→ 3)-[α-D-Gal*p*-(1 → 6)]-α-D-Glc*p*-(1 → 3)-β-D-Glc*p*-(1 → 3)-α-D-Gal*p*A-(1 → 3)-α-D-Man*p*-(1 →

The comparison of the TOCSY and HMQC–TOCSY spectra of this sample with those of the intact polysaccharide gave the position of the minor acetyl groups (Fig. 1), which produced microhetero-

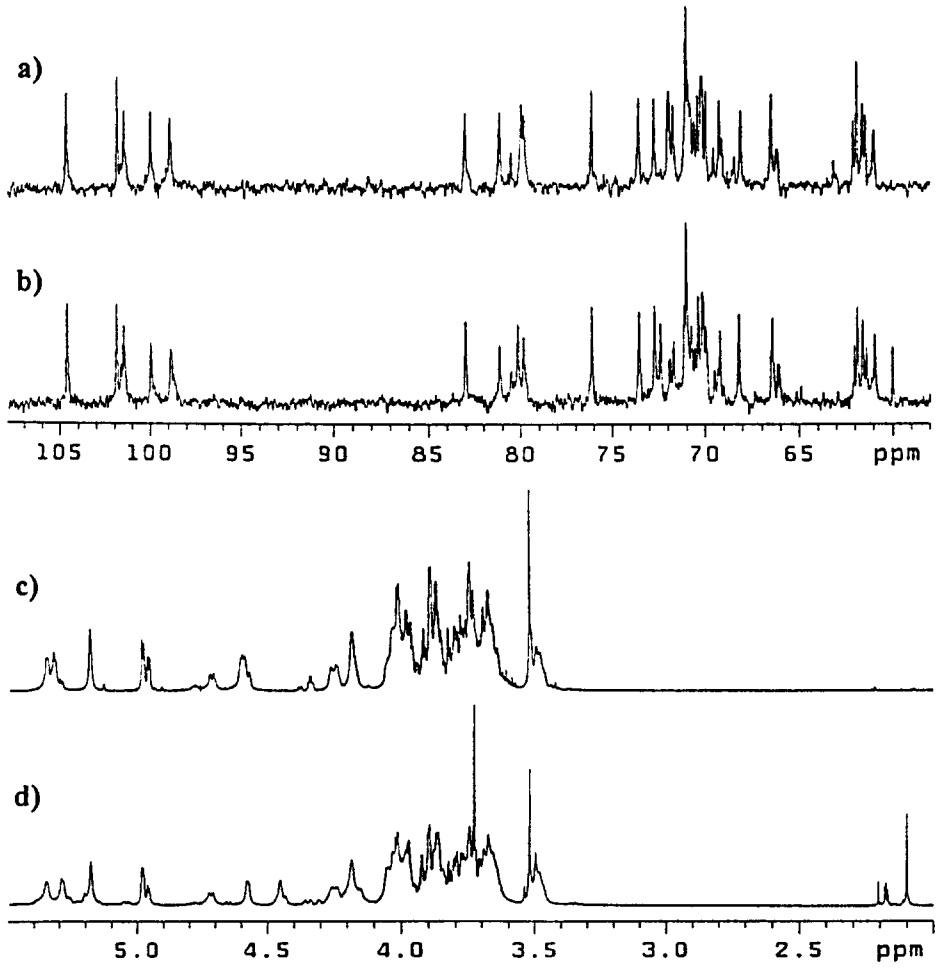

Fig. 1. ^{13}C NMR spectra at 125 MHz of the deacetylated (a) and acetylated (b) polysaccharide isolated from *Bradyrhizobium*. ^{1}H NMR spectra at 500 MHz of the deacetylated (c) and acetylated (d) polysaccharide isolated from *Bradyrhizobium*. Solvent is D_2O and temperature, 299 K.

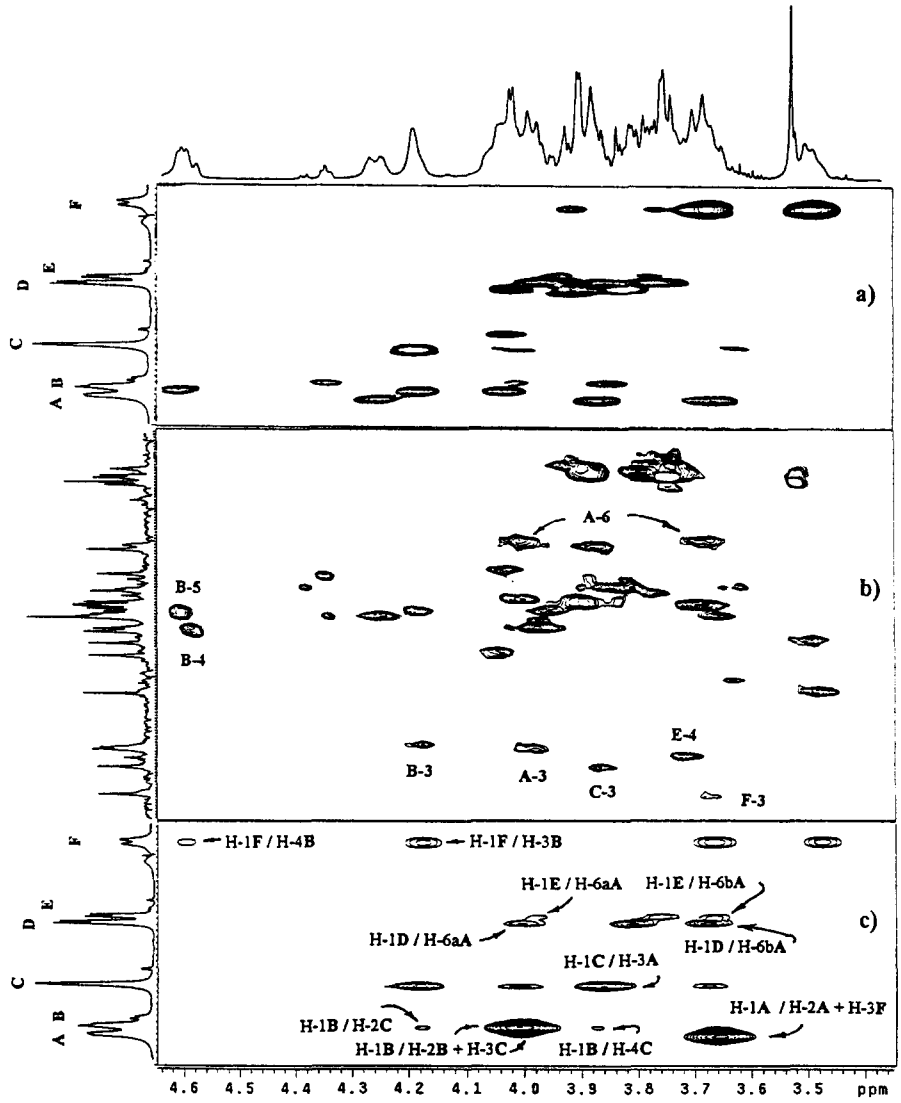

Fig. 2. Key regions of the TOCSY (a), HMQC (b), and NOESY (c) 500 MHz spectra (mixing time 500 ms) of the deacetylated polysaccharide isolated from *Bradyrhizobium* at 299 K in D_2O.

genity: Cross peaks from the D and E anomeric signals (ca. 4.95 ppm) to protons at 4.57 and 4.44 ppm appear in the TOCSY spectrum of the acetylated sample. These cross peaks disappear when deacetylation takes place. Integration of the signal corresponding to the O-acetyl groups indicated that these were present in even smaller amounts than the OMe moiety (Fig. 1), and since they are present in an heterogeneous manner, no attempts were performed to further characterize all their positions [15]. Thus, all the minor OMe and OAc substituents, which are the origin of the observed microheterogeneity, are included in the α-D-Gal*p* residue. A similar structure, with acetyl groups at the GalA moiety has been previously found in the extracellular polysaccharide produced by the bacterium *Rhizobium japonicum* [3,16] by means of chemical and glycosidase hydrolysis, ^{1}H-NMR spectroscopy and methylation analysis.

Conformational analysis.— Molecular dynamics studies.—In a first step to determine the overall three dimensional structure of the deacetylated polysaccharide within a global project directed towards the understanding of its metal binding properties, molecular mechanics and dynamics calculations were performed. Information on the accessible amount of conformational space was obtained through molecular mechanics calculations and MD simulations [17] of fragments of the polysaccharide. In vacuo simulations with the DISCOVER–CVFF and MM3* programmes were performed, since they have provided satisfactory results in the study of the conformation of a variety of oligosaccharide molecules [18]. First,

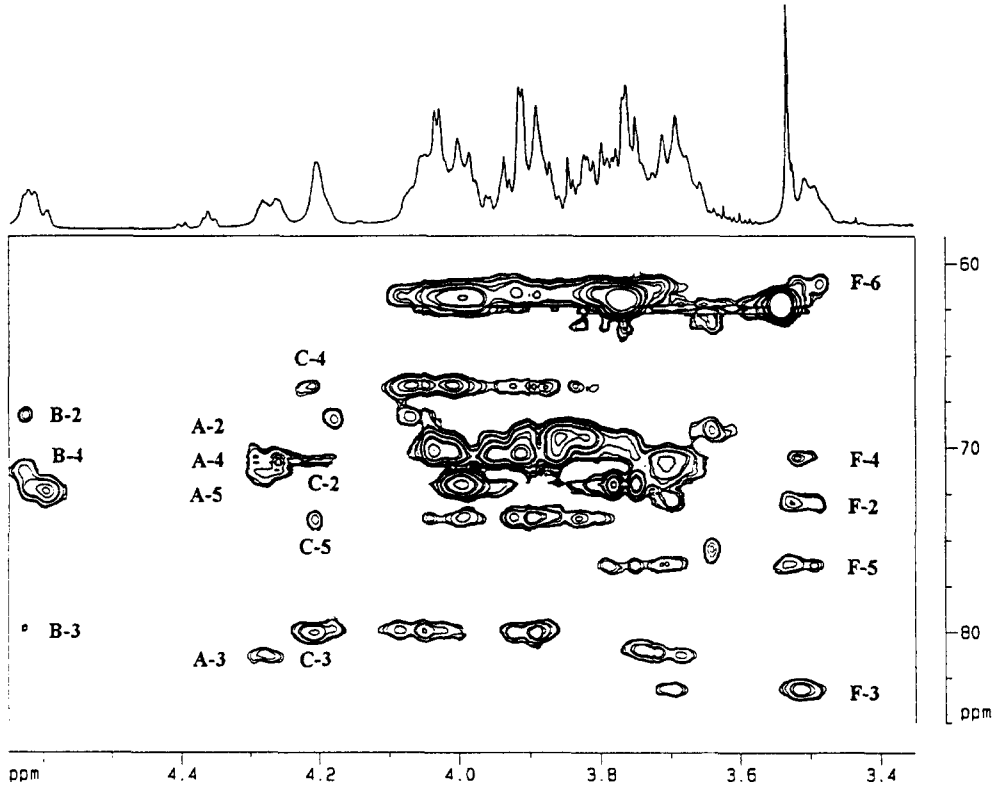

Fig. 3. Expansion of the HMQC–TOCSY spectrum obtained for the deacetylated polysaccharide isolated from *Bradyrhizobium* at 299 K in D_2O.

relaxed potential energy maps (Φ–Ψ) were calculated for every glycosidic linkage. All the glycosidic linkages present well defined low energy regions, which cover, in all cases, less than 20% of the complete potential energy surface. All the energy regions show Φ values (Table 2) which are centred around those expected for the *exo*-anomeric effect [19], although the expected probability distributions occupy a wide surface. Table 3 shows the associated

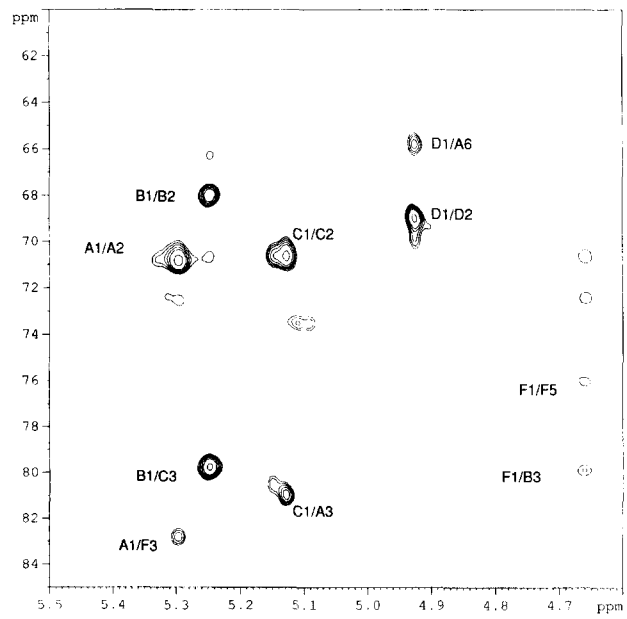

Fig. 4. Expansion of the HMQC–NOESY spectrum obtained for the deacetylated polysaccharide isolated from *Bradyrhizobium* at 299 K in D_2O.

Table 1
^{1}H- and ^{13}C-NMR chemical shifts of the deacetylated polysaccharide isolated from *Rhizobium* at 299 K in D_2O

Atom	Residue					
	A	B	C	D	E	F
H-1	5.35	5.32	5.18	4.98	4.96	4.71
H-2	3.65	4.02	4.17	3.82	3.76	3.48
H-3	3.85	4.17	3.97	3.88		3.66
H-4	3.65	4.59	3.86		3.72	3.67
H-5	4.24	4.59	4.03	3.96	3.94	3.47
H-6A	3.99	–	3.87	3.86	3.88	3.91
H-6B	3.66	–	3.74	3.76	3.74	3.74
C-1	100.1	101.6	101.9	99.0	99.0	104.7
C-2	71.2	68.0	70.6	69.1	69.4	72.9
C-3	81.2	79.8	80.0	70.4	70.4	83.0
C-4	71.2	70.6	66.4	70.0	80.4	70.4
C-5	71.2	71.2	73.7	71.8	72.0	76.2
C-6	66.2	175.0	61.6	61.8	61.8	61.2

Table 2
Torsion angles for the global minima of the constituent disaccharide entities of the polysaccharide, as calculated by the MM3* program

Fragment	MM–MM3* Φ/Ψ	MD–MM3* Φ/Ψ	MD–CVFF Φ/Ψ
Man–Glcα	−55/−40	−50 ± 30/10 ± 60	−40 ± 35/−5 ± 40
Glcα–Glcβ	−50/−35	−50 ± 20/−10 ± 60	−50 ± 15/−5 ± 20
Glcβ–GlcA	55/20	65 ± 25/20 ± 50	15 ± 25/−10 ± 15
GlcA–Man	−45/−30	−55 ± 20/0 ± 70	−50 ± 10/15 ± 20
Gal–Glcα	−50/−170	−50 ± 25/180 ± 25	−50 ± 25/−165 ± 25

The average interglycosidic torsion angles (and oscillations) found during CVFF and MM3* molecular dynamics simulations of hepta- and nona-saccharide fragments of the polysaccharide are also given.

relevant proton/proton interresidue distances of the different maps which may be correlated with experimental NOE information [20]. In addition, a nonasaccharide model of the polysaccharide was built, composed of all the different glycosidic linkages of the polysaccharide, and submitted to different 1 ns simulations using again both force fields (see experimental). For all linkages, the glycosidic torsion angles cover a well defined part of the complete Φ–Ψ map, which is fairly independent of the rotamer present at the hydroxymethyl group of the branched α-Glc moiety. Independently of the force fields used, for the α-linkages, the glycosidic torsion angles Φ and Ψ show oscillations around −60 and 0 degrees, respectively as observed in Table 2. On the other hand, for the β-D-Glc*p*-(1 → 3)-α-D-Gal*p*A linkage, Φ and Ψ present variations centred at 60 and 0 degrees for the MM3* simulations. On the other hand, the CVFF simulation presents Φ values centred around −15 degrees (supporting information). Nevertheless, it has to be mentioned that this value also belongs to the low energy region. In all cases, these torsional oscillations are more pronounced around Ψ, as expected by the operativity of the *exo*-anomeric effect around Φ. In terms of the available space for the interglycosidic torsion angles, the calculated results are fairly similar for the different α-(1 → 3)-linkages, almost independently of the nature of the aglycon. With respect to the accessible conformational space for the α-Gal*p*-(1 → 6)-α-Glc*p* linkage, the observed results are also independent on the conformation (*gg* or *gt*) of the exocyclic chain and indicate a larger accessible area of conformational space, as expected for α-(1 → 6)-linkages. In most of the cases, several transitions between the rotamers of the hydroxymethyl group were observed. Nevertheless, the hydroxymethyl

Table 3
Comparison of the molecular mechanics and dynamics calculated proton–proton interresidue distances with those estimated experimentally from NOESY and ROESY cross relaxation rates

Proton pair	Calculated distances (Å)			Experimental (Å)	
	MM3 (gt)	MD–MM3	MD–CVFF	NOE	ROE
H-1Gal–H-6aGlcα	2.42	2.92	2.56	2.85–2.96	2.59–2.61
H–1Gal–H-6bGlcα	2.89	2.36	2.88	3.10–3.32	2.67–2.72
H-1Gal–H-5Glcα	3.28	4.66	4.52	> 3.5	3.21–3.27
H-1Man–H-2Glcα	4.15	4.22	4.54	3.37–3.60	3.70–3.80
H-1Man–H-3Glcα	2.69	2.55	2.42	2.35–2.36	2.30–2.35
H-1Man–H-4Glcα	3.15	3.15	3.88	> 3.5	> 3.5
H-1Glcα–H-2Glcβ	4.14	4.36	4.56	overlapping	overlapping
H-1Glcα–H-3Glcβ	2.57	2.59	2.39	< 2.3	< 2.3
H-1Glcα–H-4Glcβ	3.17	3.13	3.91	> 3.5	> 3.5
H-1Glcβ–H-2GalA	3.26	3.44	4.44	2.90–3.67	2.95–3.72
H-1Glcβ–H-3GalA	2.60	2.57	2.19	2.21–2.50	2.23–2.41
H-1Glcβ–H-4GalA	4.21	4.21	4.10	> 3.5	> 3.5
H-1GalA–H-2Man	3.61	3.61	3.73	overlapping	overlapping
H-1GalA–H-3Man	2.55	2.55	2.32	< 2.3	< 2.3
H-1GalA–H-4Man	3.30	3.30	4.33	> 3.5	> 3.5

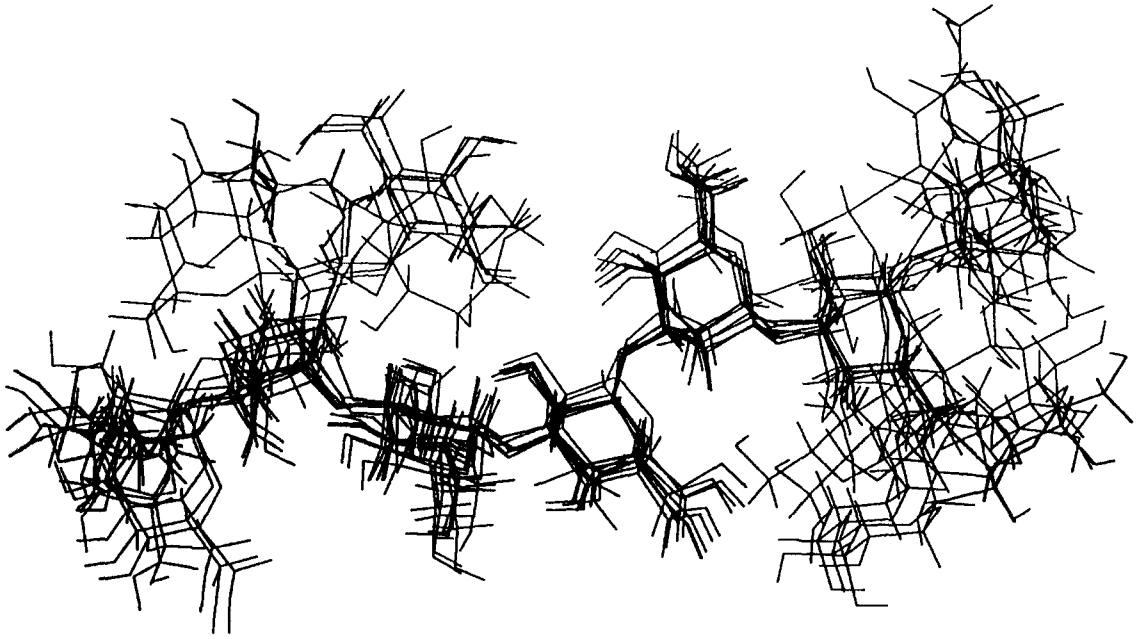

Fig. 5. Superimposition of eight different snapshots taken from the in vacuo MD simulations performed for a nonasaccharide fragment of the polysaccharide. The existence of an important amount of flexibility around the glycosidic linkages is evident.

groups displayed either the *gg* or the *gt* conformations for most of the simulation time (> 90%, [21]) Finally, average expected interproton distances from the different MD simulations (Table 3) were estimated and compared to those observed experimentally. No close proton–proton distances were deduced from the MD models which were not apparent in the experimental NOE data.

A superimposition of different conformers found in the MD simulation is shown in Fig. 5.

^{1}H-NMR DATA.—NOESY and ROESY experiments were used to qualitatively estimate proton/proton interresidue distances [22]. At 299 K, NOESY cross peaks are negative (Fig. 2) at both 300 and 500 MHz. The isolated spin pair approximation was used to estimate proton–proton distances from both sets of experiments (NOESY and ROESY) in an independent way (Table 2). The corresponding H-1/H-2 intraresidue signals were used as reference for the α-linkages, and the H-1/H-3 and H-1/H-5 intensities, for the unique β-linkage. Since overlap between key protons was observed for H-2A and H-3 F, HMQC–NOESY experiments (Fig. 4) were performed. DANTE-Z based pseudo-3D selective 1D-TOCSY–NOESY experiments [23] following the pathways H-1 F-(TOCSY) → H-3 F-(NOESY) → H-1 and H-1 A-(TOCSY) → H-2 A-(NOESY) → H-1 A were also carried out in order to get qualitative information. The estimated experimental distances are shown in Table 3. It can be observed that a good match is observed between the distances found experimentally and those estimated through molecular mechanics and dynamics simulations. The results obtained may indicate that, as least for this particular case, these unrestrained MD simulations [24] provide a fair description of the motion around the different glycosidic linkages of this molecule.

Therefore, and summarizing the theoretical and experimental results, it seems that there is an important amount of conformational freedom for the glycosidic and exocyclic torsion angles of this polysaccharide, although a representative major conformer may be deduced from Fig. 5.

Acknowledgements

Financial support of DGICYT (project PB93-0172) is gratefully acknowledged. The work of M.S. and J.C. was supported by a grant from the Canary Islands Government. We thank Prof. Martín-Lomas for his interest and the SIdI-UAM for the facilities provided throughout this work.

References

[1] A.J. Mort and W.D. Bauer, *Plant Physiol.* 66 (1980) 158–163.

[2] J. Corzo, M. León-Barrios, V. Hernando-Rico, and A.M. Gutiérrez-Navarro, *Appl. Environ. Microbiol.*, 60 (1994) 4531–4536.
[3] A.J. Mort and W.D. Bauer, *J. Biol. Chem.*, 257 (1982) 1870–1875.
[4] J.L. Geddie and I.L. Sutherland, *J. Appl. Bacteriol.*, 74 (1993) 467–472.
[5] R.Y. Taylor and H.E. Conrad, *Biochemistry*, 11 (1972) 1383–1388.
[6] Y. Ciucanu and F. Kerek, *Carbohydr. Res.*, 131 (1984) 209–217.
[7] A.T. Hagler, S. Lifson, and P. Dauber, *J. Am. Chem. Soc.*, 101 (1979) 512 [4].
[8] F. Mohamadi, N.G.I. Richards, W.C. Guida, R. Liskamp, C. Canfield, G. Chang, T. Hendrickson, and W.C. Still, *J. Comput. Chem.*, 11 (1990) 440–467.
[9] A.D. French and J.D. Brady, *ACS Symp. Ser.*, 430 (1990) 1. (a) C. Meyer, S. Perez, C. Herve du Penhoat, and V. Michon, *J. Am. Chem. Soc.*, 115 (1993) 10300–10310. (b) S.B. Engelsen, C. Herve du Penhoat, and S. Perez, *J. Phys. Chem.*, 99 (1995) 13334–13351. (c) R.U. Lemieux, *Chem. Soc. Rev.*, 18 (1989) 347–374. (d) K. Bock, *Pure Appl. Chem.*, 55 (1983) 605–622.
[10] (a) J.P. Carver, *Pure Appl. Chem.*, 65 (1993) 763–770 (b) D.A. Cumming and J.P. Carver, *Biochemistry*, 26 (1987) 6664–6676.
[11] (a) S.W. Homans, *Biochemistry*, 29 (1990) 9110–9118; (b) B.J. Hardy, W. Egan, and G. Widmalm, *Int. J. Biol. Macromol.*, 17–18 (1995) 149–60; (c) C.J. Edge, U.C. Singh, R. Bazzo, G.L. Taylor, R.A. Dwek, and T.W. Rademacher, *Biochemistry*, 29 (1990) 1971–1974; (d) P.J. Hajduk, D.A. Horita, and L. Lerner, *J. Am. Chem. Soc.* 115 (1993) 9196–201; (e) T.J. Rutherford, D.G. Spackman, P.J. Simpson, and S.W. Homans, *Glycobiology*, 4 (1994) 59–68; (f) A. Poveda, J.L. Asensio, M. Martin-Pastor, and J. Jimenez-Barbero, *Chem. Comm.* (1996) 421–422.
[12] (a) C.A. Bush, *Curr. Opin. Struct. Biol.*, 2 (1992) 655–663; (b) H. van Halbeek, *Curr. Opin. Struct. Biol.*, 4 (1994) 697–709; (c) J. Jimenez-Barbero, M. Bernabe, J.A. Leal, A. Prieto, and B. Gomez-Miranda, *Carbohydr. Res.*, 250 (1993) 289–299.
[13] D. Boudot, D. Canet, J. Brondeau, and J.C. Boubel, *J. Magn. Res.*, 83 (1989) 428.
[14] K. Bock, C. Pedersen, and H. Pedersen, *Adv. Carbohydr. Chem. Biochem.*, 42 (1984) 193–225.
[15] (a) T.J. Rutherford, C. Jones, D.B. Davies, and A.C. Elliot, *Carbohydr. Res.*, 218 (1991) 175–184; (b) X. Lemercinier and C. Jones, *Carbohydr. Res.*, 296 (1996) 83–96.
[16] W.F. Dudman, *Carbohydr. Res.*, 46 (1976) 97–110.
[17] (a) A. Ejchart, J. Dabrowski, and C.-W. von der Lieth, *Magn. Res. Chem.*, 30 (1992) S105–S114; (b) C. Mukhopadhyay, K.E. Miller, and C.A. Bush, *Biopolymers*, 34 (1994) 21–29; (c) T.J. Rutherford, J. Partridge, C.T. Weller, and S.W. Homans, *Biochemistry*, 32 (1993) 12715–12724.
[18] (a) H.C. Siebert, G. Reuter, R. Schauer, C.W. von der Lieth, and J. Dabrowski, *Biochemistry*, 31 (1992) 6962–6971; (b) J.L. Asensio, M. Martín-Pastor, and J. Jimenez-Barbero, *Int. J. Biol. Macromol.*, 17 (1995) 52–55; (c) J.M. Coteron, K. Singh, J.L. Asensio, M.D. Dalda, A. Fernández-Mayoralas, J. Jiménez-Barbero, and M. Martín-Lomas, *J. Org. Chem.*, 60 (1995) 1502–1513; (d) M.K. Dowd, P.J. Reilly, and A.D. French, *J. Comput. Chem.*, 13 (1992) 102–114; (e) J.F. Espinosa, J.L. Asensio, M. Bruix, and J. Jimenez-Barbero, *Ann. Quim. Int. Ed.*, 96 (1996) 320–324.
[19] R.U. Lemieux, K. Bock, L.T.J. Delbaere, S. Koto, and V.S. Rao, *Can. J. Chem.*, 58 (1980) 631–653.
[20] (a) B.R. Leeflang and L.M.J. Kroon-Batenburg, *J. Biomol. NMR*, 2 (1992) 495–518; (b) J.P.M. Lommersee, L.M.J. Kroon-Batenburg, J. Kron, J.P. Kamerling, and J.F.G. Vliegenthart, *J. Biomol. NMR*, 5 (1995) 79–94; (c) T. Peters and T. Weimar, *J. Biomol. NMR*, 4 (1994) 97–116; (d) K.G. Rice, P. Wu, L. Brand, and Y.C. Lee, *Curr. Opin. Struct. Biol.*, 3 (1993) 669–674.
[21] K. Bock and J. Duus, *J. Carbohydr. Chem.*, 13 (1994) 513–543.
[22] D. Neuhaus and M.P. Williamson, *The Nuclear Overhauser Effect in Structural and Conformational Analysis*; VCH, New York, 1989.
[23] D. Uhrin, J.R. Brisson, and D.R. Bundle, *J. Biomol. NMR*, 3 (1993) 367–373.
[24] (a) T.J. Rutherford and S.W. Homans, *Biochemistry*, 33 (1994) 9606–9614; (b) T.J. Rutherford, D.C.A. Neville, and S.W. Homans, *Biochemistry*, 34 (1995) 14131–14137.